Author(s): Altowyan, Mezna Saleh; Haukka, Matti; Soliman, Saied M.; Barakat, Assem; Boraei, Ahmed T. A.; Aboelmagd, Ahmed

Title: Stereoselective Synthesis of New 4-Aryl-5-indolyl-1,2,4-triazole S- and N-β-Galactosides : Characterizations, X-ray Crystal Structure and Hirshfeld Surface Analysis

Year: 2023

Version: Published version

Please cite the original version:

Altowyan, M. S., Haukka, M., Soliman, S. M., Barakat, A., Boraei, A. T. A., & Aboelmagd, A. (2023). Stereoselective Synthesis of New 4-Aryl-5-indolyl-1,2,4-triazole S- and N-β-Galactosides : Characterizations, X-ray Crystal Structure and Hirshfeld Surface Analysis. Crystals, 13(5), Article 797. https://doi.org/10.3390/cryst13050797

crystals

MDPI

Article

Stereoselective Synthesis of New 4-Aryl-5-indolyl-1,2,4-triazole *S*- and *N*-β-Galactosides: Characterizations, X-ray Crystal Structure and Hirshfeld Surface Analysis

Mezna Saleh Altowyan [1], Matti Haukka [2], Saied M. Soliman [3], Assem Barakat [4,*], Ahmed T. A. Boraei [5] and Ahmed Aboelmagd [5,*]

[1] Department of Chemistry, College of Science, Princess Nourah bint Abdulrahman University, P.O. Box 84428, Riyadh 11671, Saudi Arabia; msaltowyan@pnu.edu.sa
[2] Department of Chemistry, University of Jyväskylä, P.O. Box 35, FI-40014 Jyväskylä, Finland; matti.o.haukka@jyu.fi
[3] Chemistry Department, Faculty of Science, Alexandria University, P.O. Box 426, Alexandria 21321, Egypt; saeed.soliman@alexu.edu.eg
[4] Department of Chemistry, College of Science, King Saud University, P.O. Box 2455, Riyadh 11451, Saudi Arabia
[5] Chemistry Department, Faculty of Science, Suez Canal University, Ismailia 41522, Egypt; ahmed_tawfeek83@yahoo.com
* Correspondence: ambarakat@ksu.edu.sa (A.B.); ah_abuoelmaged@hotmail.com or ahmed_mohamed@science.suez.edu.eg (A.A.); Tel.: +966-11467-5901 (A.B.); Fax: +966-11467-5992 (A.B.)

Abstract: 5-(1*H*-Indol-2-yl)-4-phenyl-2,4-dihydro-3*H*-1,2,4-triazole-3-thione **1a** and 4-(4-chlorophenyl)-5-(1*H*-indol-2-yl)-2,4-dihydro-3*H*-1,2,4-triazole-3-thione **1b** were galactosylated in the presence of $NaHCO_3$ in ethanol to produce *S*-galactosides **3,4**, whereas, in the presence of K_2CO_3 in acetone they produced a mixture of *S*- and *N*-galactosides **3-6** with a higher yield of *S*-galactosides over the respective *N*-galactosides. Improvement in the yields of *N*-galactosides was produced by thermal migration of the galactosyl moiety from sulfur to nitrogen using fusion. β-Stereoselectivity of galactosylation was determined using the coupling constant value $^3J_{1,2}$, which exceeded 9.0 Hz in all prepared galactosides. The precursors **1a** and **1b** alkylated with 3-bromopropan-1-ol **7** in K_2CO_3 and acetone produced the *S*-alkylated products **8** and **9**, respectively. Structural determinations of new compounds **5** and **9** are presented. The phenyl and indole moieties were found to be twisted from the triazole ring mean in both compounds. For compound **5**, the twist angles were 66.24° and 18.86°, respectively, while the corresponding values for **9** were in the ranges of 73.15–77.29° and 13.96–20.70°, respectively. Hence, the crystal system of **9** is triclinic while the space group is *P-1*. Detailed analysis of the intermolecular interactions in the crystal structure of **5** is presented using Hirshfeld calculations. The O ... H, N ... H, C ... H, and S ... H contacts appeared as red spots in the d_{norm} Hirshfeld surface indicating short distance intermolecular interactions. Their percentages were estimated based on the decomposition of the fingerprint plot to be 25.6, 2.4, 14.0, and 6.3%, respectively.

Keywords: indole; 1,2,4-triazole; galactoside; X-ray single crystal; Hirshfeld surface

Citation: Altowyan, M.S.; Haukka, M.; Soliman, S.M.; Barakat, A.; Boraei, A.T.A.; Aboelmagd, A. Stereoselective Synthesis of New 4-Aryl-5-indolyl-1,2,4-triazole *S*- and *N*-β-Galactosides: Characterizations, X-ray Crystal Structure and Hirshfeld Surface Analysis. *Crystals* **2023**, *13*, 797. https://doi.org/10.3390/cryst13050797

Academic Editor: Volodymyr Bon

Received: 27 April 2023
Revised: 3 May 2023
Accepted: 5 May 2023
Published: 10 May 2023

1. Introduction

Due to the major role that glycosides, glycoconjugates, and nucleosides play in biological processes, the discovery of such molecules is necessary. These compounds with complex structures, diverse stereochemistry, and numerous linkage possibilities are qualified to fulfill many different functions in biological systems [1]. Indole moiety is one of the most potent pharmacophores, and it constitutes the backbones of serotonin (neurotransmitter) and melatonin (natural hormone), in addition to tryptophan (an essential amino acid). Mitomycin and its analogues are bioactive indole alkaloids gaining great attention because of their use in cancer chemotherapy and in treatment of bacterial infections [2,3]. Moreover, compounds containing an indole nucleus are significant regarding the improvement of various bioactive compounds through derivatization or substitution at the indole ring.

These compounds exhibit various biological activities such as antimicrobial, antiviral, anticonvulsant, analgesic, anti-inflammatory, antitubercular, and anticancer effects [4–8].

The 1,2,4-Triazole nucleus also acts as an important pharmacophore, which is characterized by a high affinity for interacting with biological receptors due to its hydrogen bonding capacity, dipole character, solubility, and rigidity [9]. Due to its polar nature, the triazole nucleus could increase the solubility of ligands and considerably improve the pharmacological features of the drug [10]. Many anticancer agents such as tebuconazole, triadimefon, fluconazole, and ribavirin have a 1,2,4-triazole moiety [11]. The 1,2,4-Triazole-3-thiones/thiols show more potency associated to their parent compounds [12]. They have shown interesting biological activities, such as antimicrobial, anticancer, antitubercular, and hypoglycemic properties [13–15].

Triazole heterocycles, which incorporate exocyclic sulfur as mercapto (thiols) and thiones, reveal more potency compared to their parent compounds [12]. A diversity of biological activities was found for 1,2,4-triazole-3-thione and 1,2,4-triazole-3-thiol, including anticancer, antimicrobial, antitubercular, and hypoglycemic activities [13–15]. Carbohydrates possess essential roles in nature by means of being energy sources and structural matter, and because of their molecular recognition in cellular processes [16]. Hence, bringing indole, 1,2,4-triazole, and carbohydrate or alkyl groups into a single heterocyclic framework could result in enhancing biological properties [17–21]. Maftei, et al. combined a pyrazole–pyrimidine unit with 1,2,4-oxadiazole and trifluoromethylpyridine moieties to improve the antitumor activity of the heterocyclic system as whole [22]. A galactosylation reaction means a coupling of a galactcosyl donor with a galactosyl acceptor to form galactoside. A galactosyl donor with a suitable leaving group at the anomeric position is required. Neda, et al. successfully used 2,3,4,6-tetra-*O*-benzyl-*β*-D-galactopyranosyl difluorophosphate as a galactosyl donor for the synthesis of highly *β*-stereoselective galactosylation [23]. Herein, a 2,3,4,6-tetra-*O*-acetyl-α-D-galactopyranosyl bromide galactosyl donor was used.

In organic and bio-organic chemistry, the determination of structural features such as the site of alkylation (i.e., whether the alkylation is performed on sulfur or nitrogen) and the configuration of the glycosyl moiety (alpha or beta) is very significant for recognizing a structure's activity relationship and pharmacological action. In this context, *S*-, *N*-*β*-D-galactosides and exocyclic 3-hydroxyproyl derivatives as acyclonucleosides were synthesized. The chemical structures, galactosyl moiety configuration, and site of alkylation were assigned using NMR. In addition, X-ray single crystal analysis was used for studying the crystal features of compounds **5** and **9**. Moreover, full analysis of intermolecular interactions that control molecular packing in crystal structures was performed using Hirshfeld surface calculations.

2. Materials and Methods

2.1. Chemicals and Instrumentation

Anhydrous solvents and all reagents were purchased from Sigma-Merck (Haverhill, MA, USA) and Alfa Aesar (Mississauga, ON, Canada). Melting points were measured via a melting-point apparatus (SMP10, Starfire Systems Inc., Schenectady, NY, USA) in open capillaries and were uncorrected. The progress of the reactions was observed using thin layer chromatography (TLC) with pre-coated plates with silica gel 60 F254 with a thickness of 0.25 mm (Merck, Millipore, Burlington, MA, USA). Detections were achieved using UV light illumination and/or treatment with a solution of 10% H_2SO_4 in aqueous methanol. For flash chromatography, commercial alumina or silica was used. Nuclear magnetic resonance (^{1}H NMR and ^{13}C NMR) spectra were determined in $CDCl_3$ and DMSO-d_6 and were recorded on a Bruker AC 400 MHz spectrometer (Bremen, Germany) in the presence of tetramethylsilane as an internal standard. Chemical shifts were described in δ (ppm), and coupling constants were given in Hz. EI mass spectra were recorded with Finnigan MAT312 and Jeol JMS.600H (Tokyo, Japan) mass spectrometers. HREI mass spectra were recorded with a Finnigan MAT 95XP instrument. ESI-MS spectra were recorded with an Applied BiosystemsQStar XL apparatus (Darmstadt, Germany).

2.2. General Procedures for Galactosylation

2.2.1. Method A

To a solution of the selected 4-aryl-1,2,4-triazole-thione **1a** or **1b** (1.0 mmol) in dry acetone (10 mL), K_2CO_3 (1.1 mmol), was added. After stirring the previous mixture for one hour, 2,3,4,6-tetra-*O*-acetyl-*α*-D-galactopyranosyl bromide (1.1 mmol) was added portion-wise and the reaction mixture kept overnight under continuously stirring. The solvent was evaporated under vacuum; then, cold water was added, and the formed precipitate was collected and dried. Pure products were separated using alumina column chromatography with elution using ethyl acetate/n-hexane 3:7.

2.2.2. Method B

A mixture of the selected 4-aryl-1,2,4-triazole-thione **1a** or **1b** (1.0 mmol) and $NaHCO_3$ (1.1 mmol), in abs. EtOH (10 mL), was stirred for one hour; then, 2,3,4,6-tetra-*O*-acetyl-*α*-D-galactopyranosyl bromide (1.1 mmol) was added portion-wise, and the mixture was continuously stirred for 48 h. The workup was performed as in method A.

2.3. General Method for Thermal Transformation of S-Galactosides into N-Glycosides

Method C

The *S*-galactosides **3,4** (0.1 mmol) were heated on a hotplate at a temperature a little bit higher than the melting point for 5 min; TLC was used to follow up the conversion process. The fused mass was allowed to cool to room temperature once galactosyl migration was finished, and the resulting solid was powdered and recrystallized from EtOH to provide the corresponding N-galactosides **5,6**.

5-(1*H*-Indol-2-yl)-4-phenyl-3-(2,3,4,,6-tetra-*O*-acetyl-*β*-D-galactopyranosylsulfanyl)-1,2,4-triazole 3. Yields: (66% method A, 65% method B), m.p. 138–140 °C. ^{1}H NMR (400 MHz, $CDCl_3$): δ 1.94, 2.00, 2.05, 2.13 (4s, 12H), 4.08–4.13 (m, 3H), 5.13–5.20 (m, 1H), 5.13 (t, 1H, *J* = 10.0 Hz), 5.47 (s, 1H), 5.68 (d, 1H, *J* = 10.20 Hz), 5.74 (s, 1H), 7.03 (dd, 1H, *J* = 7.6, *J* = 7.2 Hz), 7.21 (t, 1H, *J* = 7.6 Hz), 7.35–7.45 (m, 3H), 7.62–7.71 (m, 4H), 11.17 (br.s, 1H); ^{13}C NMR (100 MHz, $CDCl_3$): δ 20.57, 20.59, 20.63, 20.74, 61.24, 67.18, 67.31, 71.71, 74.90, 84.86, 103.37, 112.28, 120.37, 121.21, 123.04, 124.07, 127.68, 127.99, 130.33, 131.00, 133.40, 136.91, 149.58, 150.27, 169.83, 169.90, 170.23, 170.37; HRMS (EI): m/z Calcd for $C_{30}H_{30}N_4O_9S$ (M+): 622.1733 Found: 622.1733.

4-(4-Chlorophenyl)-5-(1*H*-indol-2-yl)-3-(2,3,4,,6-tetra-*O*-acetyl-*β*-D-galactopyranosylsulfanyl)-1,2,4-triazole 4. Yields: (67% method A, 69% method B), m.p. 154–155 °C. ^{1}H NMR (300 MHz, $CDCl_3$): δ 1.94, 2.00, 2.07, 2.15 (4s, 12H), 4.08–4.13 (m, 3H), 5.17 (dd, 1H, *J* = 10.00, *J* = 3.20 Hz), 5.31 (t, 1H, *J* = 10.0 Hz), 5.47 (d, 1H, *J* = 3.20 Hz), 5.64 (d, 1H, *J* = 10.0 Hz), 5.80 (s, 1H), 7.05 (dd, 1H, *J* = 7.6, *J* = 7.2 Hz), 7.22 (dd, 1H, *J* = 7.20, *J* = 8.00 Hz), 7.34–7.37 (m, 2H), 7.44 (d, 1H, *J* = 8.0 Hz), 7.60–7.65 (m, 3H), 10.93 (br.s, 1H); ^{13}C NMR (75 MHz, $CDCl_3$): δ 20.55, 20.61, 20.71, 61.29, 67.24, 67.39, 71.63, 74.98, 85.13, 103.34, 112.24, 120.48, 121.27, 122.83, 124.18, 127.64, 129.44, 130.59, 131.88, 136.91, 137.15, 149.44, 150.16, 169.83, 169.87, 170.19, 170.32; HRMS (ESI +ve mode): m/z Calcd for $C_{30}H_{29}N_4O_9SCl$ (M + 1): 657.1422 Found: 657.1360.

5-(1*H*-Indol-2-yl)-4-phenyl-2-(2,3,4,6-tetra-*O*-acetyl-*β*-D-galactopyranosyl)-3-thioxo-1,2,4-triazole 5. Yields: (15% method A, 63% method C), m.p. > 300 °C. ^{1}H NMR (300 MHz, $CDCl_3$): δ 2.00, 2.05, 2.08, 2.29 (4s, 12H), 4.22–4.32 (m, 2H), 5.31–5.35 (m, 1H), 5.56–5.62 (m, 1H), 5.71–5.76 (m, 1H), 5.98–6.05 (m, 1H), 6.28–6.32 (m, 1H), 7.04–7.12 (m, 1H), 7.26–7.29 (m, 3H), 7.39–7.45 (m, 3H), 7.65–7.75 (m, 3H), 9.12 (br.s, 1H); ^{13}C NMR (75 MHz, $CDCl_3$): δ 20.50, 20.59, 20.68, 20.81, 61.19, 67.06, 67.33, 71.57, 73.71, 83.33, 105.80, 111.35, 120.83, 121.585, 121.73, 125.12, 127.43, 128.485, 130.23, 130.81, 134.48, 136.35, 144.73, 169.35, 169.797, 170.21, 170.36, 171.62; HRMS (EI): m/z Calcd for $C_{30}H_{30}N_4O_9S$ (M+): 622.1733. Found: 622.1723.

4-(4-Chlorophenyl)-5-(1*H*-indol-2-yl)-2-(2,3,4,,6-tetra-*O*-acetyl-*β*-D-galactopyranosyl)-3-thioxo-1,2,4-triazole 6. Yields: (18% method A, 59% method C), m.p. > 300 °C. ^{1}H NMR (300 MHz, $CDCl_3$): δ 2.00, 2.05, 2.09, 2.30 (4s, 12H), 4.22–4.29 (m, 2H), 5.32–5.35 (m, 1H), 5.58–5.62 (m, 1H), 5.81–5.84 (m, 1H), 5.96–6.02 (m, 1H), 6.24–6.27 (m, 1H), 7.09–7.13 (m, 1H), 7.28–7.30 (m, 2H), 7.43–7.48 (m, 4H), 7.62–7.68 (m, 2H), 9.15 (br.s, 1H); ^{13}C NMR (75 MHz, $CDCl_3$): δ 20.55, 20.73, 20.85, 20.89, 61.18, 66.98, 67.29, 71.51, 73.71, 83.34, 105.82, 111.40, 121.00, 121.29, 121.83, 125.33, 127.37, 129.91, 130.62, 132.85, 136.38, 137.02, 144.52, 169.42, 169.85, 170.24, 170.42, 171.52; HRMS (ESI +ve mode): m/z Calcd for $C_{30}H_{29}N_4O_9SCl$ (M + 1): 657.1422 Found 657.1330.

Alkylation with 3-bromo-1-propanol. To a solution of compound **1a** or **1b** (1.0 mmol) in dry acetone (10 mL), K_2CO_3 (1.1 mmol), was added under stirring. After one hour 3-bromo-1-propanol (1.1 mmol) was added, and the entire mixture was continuously stirred overnight. The solvent was evaporated under vacuum; then, cold water was added, and the formed precipitate was filtered, dried, and crystallized from EtOH.

3-(3-Hydroxyprop-1-ylsulfanyl)-5-(1*H*-indol-2-yl)-4-phenyl-1,2,4-triazole 8. Yield: 81%, m.p. 201–203 °C. ^{1}H NMR (DMSO-d_6, 400 MHz) δ 1.80–1.85 (m, 2H), 3.19 (t, 2H, *J* = 7.2 Hz), 3.46–3.49 (m, 2H), 4.57 (t, 1H, *J* = 5.2 Hz), 5.60 (s, 1H), 6.93 (dd, 1H, *J* = 7.6, *J* = 6.8 Hz), 7.12 (dd, 1H, *J* = 6.8, *J* = 8.0 Hz), 7.34 (d, 1H, *J* = 7.6 Hz), 7.42 (d, 1H, *J* = 8.0 Hz), 7.53–7.58 (m, 2H), 7.65–7.71 (m, 3H), 11.94 (br.s, 1H); ^{13}C NMR (DMSO-d_6, 100 MHz) δ 29.70, 32.59, 59.46, 101.77, 112.30, 120.17, 121.15, 123.54, 124.42, 127.64, 128.49, 130.70, 131.15, 134.27, 136.95, 149.55, 152.38; HRMS (EI) calcd for $C_{19}H_{18}N_4OS$ (M+): 350.1200 Found: 350.1203.

4-(4-Chlorophenyl)-3-(3-hydroxyprop-1-ylsulfanyl)-5-(1*H*-indol-2-yl)-1,2,4-triazole 9. Yield: 85 %, m.p. 214–216 °C. 1H NMR (DMSO-d_6, 400 MHz) δ 1.80–1.87 (m, 2H), 3.19 (t, 2H, *J* = 7.2 Hz), 3.46–3.50 (m, 2H), 4.58 (t, 1H, *J* = 5.2 Hz), 5.70 (s, 1H), 6.94 (dd, 1H, *J* = 7.6, J = 7.2 Hz), 7.13 (t, 1H, *J* = 7.6 Hz), 7.41–7.46 (m, 2H), 7.63 (d, 2H, *J* = 8.8 Hz), 7.75 (d, 2H, *J* = 8.8 Hz), 11.94 (br.s, 1H); ^{13}C NMR (DMSO-d_6, 100 MHz) δ 29.88, 32.58, 59.44, 101.96, 112.30, 120.20, 121.30, 123.61, 124.24, 127.69, 130.51, 130.79, 133.19, 135.78, 137.00, 149.48, 152.31; HRMS (EI) calcd for $C_{19}H_{17}N_4OSCl$ (M+): 384.0812 Found: 384.0838.

2.4. Crystal Structure Determination

The crystals of **5** and **9** were immersed in cryo-oil, mounted in a loop, and measured at a temperature of 120 K. The X-ray diffraction data were collected on a Rigaku Oxford Diffraction Supernova diffractometer using Cu Kα radiation. The CrysAlisPro [24] software package was used for cell refinements and data reductions. Gaussian absorption correction (CrysAlisPro [24]) was applied to the intensities before structure solutions. Structures were solved using the intrinsic phasing (SHELXT [25]) method. Structural refinements were carried out using SHELXL [26] software with the SHELXLE [27] graphical user interface. In **9**, the $S(CH_2)_3OH$ moieties were disordered over two sites with an occupancy ratio of 0.87/0.13. A series of geometric and displacement constraints and restraints were applied to the disordered moieties. The crystal of **9** contained solvent-containing voids. These solvent molecules could not be refined satisfactorily. Therefore, the solvent was omitted from the final refinement cycle. The contribution of the missing solvent to the calculated structure factors was taken into account by using the SOLVENT MASK routine of OLEX2 [28]. The solvent mask was calculated, and 25 electrons were found in a volume of 153 Å^3 in 1 void per unit cell. This was consistent with the presence of 2.5 H_2O per unit cell and 0.625 H_2O per formula unit, which accounted for 25 electrons per unit cell. The missing solvent was taken into account in the unit cell content. The NH hydrogen atoms were located from the difference in the Fourier map and were refined isotropically in both structures. Other hydrogen atoms were positioned geometrically and constrained to ride on their parent atoms, with C-H = 0.95–1.00 Å, O-H = 0.84 Å, and U_{iso} = 1.2–1.5·U_{eq} (parent atom). The crystallographic details are summarized in Table 1.

Table 1. Crystal data and structure refinement for the target crystals.

	5	**9**
CCDC	2243221	2243222
empirical formula	$C_{30}H_{30}N_4O_9S$	$C_{19}H_{18.25}ClN_4O_{1.625}S$
fw	622.64	396.13
temp (K)	120(2) K	120(2) K
λ (Å)	1.54184 Å	1.54184 Å
cryst syst	orthorhombic	triclinic
space group	$P2_12_12_1$	$P\bar{1}$
a (Å)	a = 6.8865(3) Å	a = 11.0384(5) Å
b (Å)	b = 13.8302(6) Å	b = 13.6634(8) Å
c (Å)	c = 32.4134(19) Å	c = 14.0630(6) Å
α (deg)	90	74.579(4)°
β (deg)	90	74.477(4)°
γ(deg)	90	72.100(5)°
V (Å^3)	3087.1(3) Å^3	1905.31(18) Å^3
Z	4	4
ρ_{calc} (Mg/m^3)	1.340 Mg/m^3	1.381 Mg/m^3
μ(Mo Kα) (mm^{-1})	1.440 mm^{-1}	2.964 mm^{-1}
no. reflns.	12175	33118
unique reflns.	6313	7107
completeness to θ=67.684°	100%	99.9%
GOOF (F^2)	1.029	1.057
R_{int}	0.0633	0.0402
R_1 [a] ($I \geq 2\sigma$)	0.0563	0.0489
wR_2 [b] ($I \geq 2\sigma$)	0.1123	0.1378

[a] $R_1 = \Sigma||F_o| - |F_c||/\Sigma|F_o|$. [b] $wR_2 = \{\Sigma[w(F_o^2 - F_c^2)^2]/\Sigma[w(F_o^2)^2]\}^{1/2}$.

2.5. Hirshfeld Surface Analysis

The topology analyses were performed using the Crystal Explorer 17.5 program [29].

3. Results and Discussion

3.1. Chemistry

The starting indolyl-triazole-thiones **1a** and **1b** were synthesized as reported in [18]. Galactosylation of the indolyl triazolethiones **1a**, **1b** with 2,3,4,6-tetra-*O*-acetyl-α-D-galactopyranosyl bromide **2** in acetone, and in presence of anhydrous K_2CO_3, afforded a mixture of two products that were separated using alumina column chromatography and characterized as *S*-galactosides **3**,**4** (yields > 65%) and the respective *N*-galactoside analogues **5**,**6** (yields < 18%). The selectivity of *S*-galactosylation was achieved using $NaHCO_3$ as a base in ethanol. The yields of *N*-galactosides **5**,**6** were improved with thermal galactosyl moiety migration from sulfur to nitrogen using simple fusion on a hotplate for few minutes without the need for a catalyst (Scheme 1). The ^{1}H NMR of the *S*-galactosides **3** and **4** showed anomeric protons around 5.64 ppm with a ^3J value of 10.2 Hz. The proton H-4 of the galactose moiety was found as a doublet near 5.47 ppm with a ^3J value of 3.2 Hz. The NH of the indole ring appeared at 10.39 and 11.17 ppm. The anomeric carbons of the *S*-galactosides **3**,**4** appeared at 84.86 and 85.13 ppm, respectively.

The ^{1}H NMR of the *N*-galactosides **5** and **6** displayed the anomeric protons at 6.28, 6.24 ppm, respectively. H-4 of galactose appeared at 5.56 and 5.58 ppm, respectively. The indole NH was found at 9.12 and 9.15 ppm. The anomeric carbons appeared at 83.33 and 83.34 ppm.

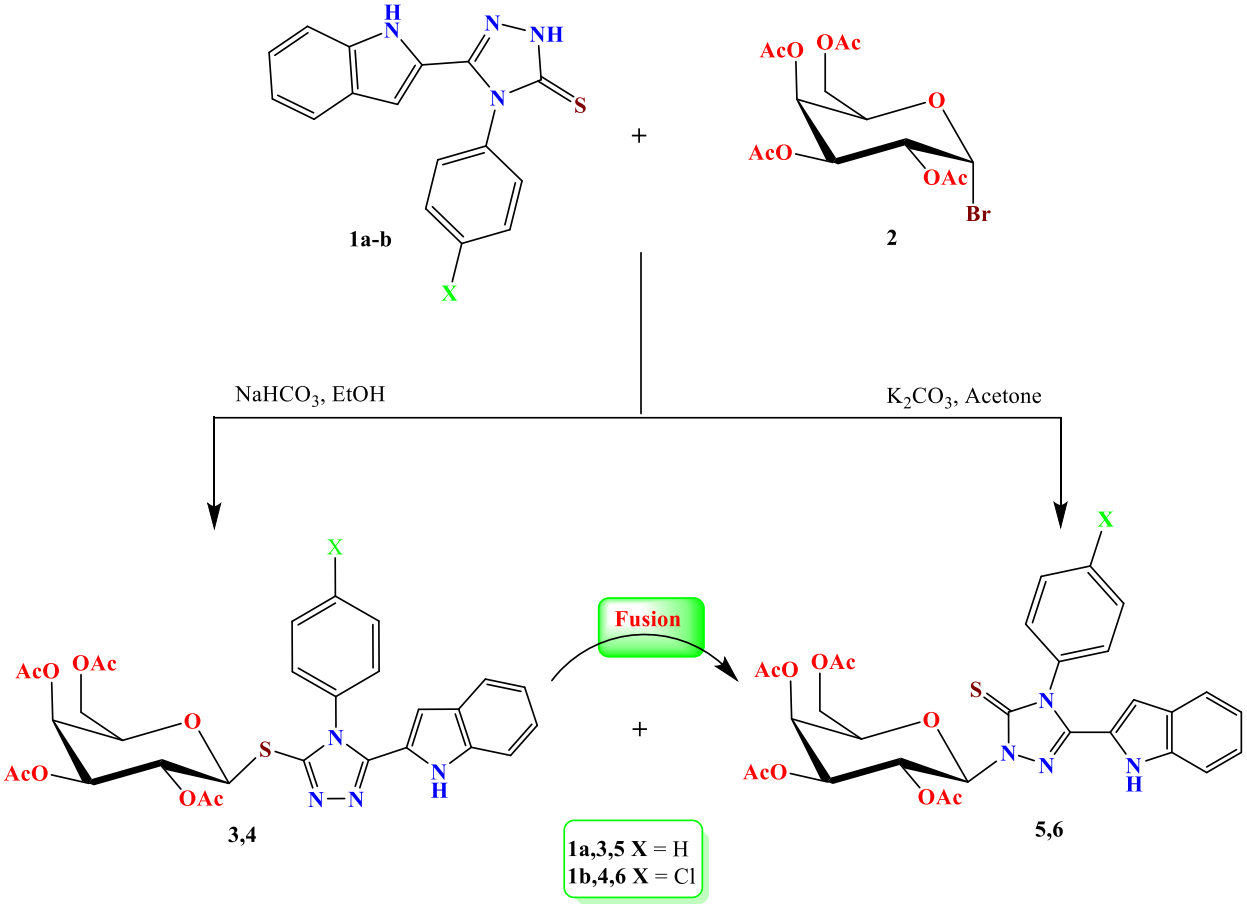

Scheme 1. Galactosylation of **1a,b**.

Alkylation of the 4-aryl-indolyl-triazoles **1a**, **1b** with 3-bromopropan-1-ol **7** in the presence of K_2CO_3 produced the respective *S*-alkylated products **8,9** (Scheme 2). The NMR of 3-hydroxypropyl-sulfanyl-triazoles **8** and **9** revealed the relative positions of three methylene group protons (-S-CH_2-CH_2-CH_2-OH) as multiplet, triplet, and multiplet at 1.80–1.85, 3.19, and 3.46–3.49 ppm, respectively. The respective methylene carbons appeared around 29.70, 32.58, and 59.44 ppm. The indole NH was found at 11.94 ppm.

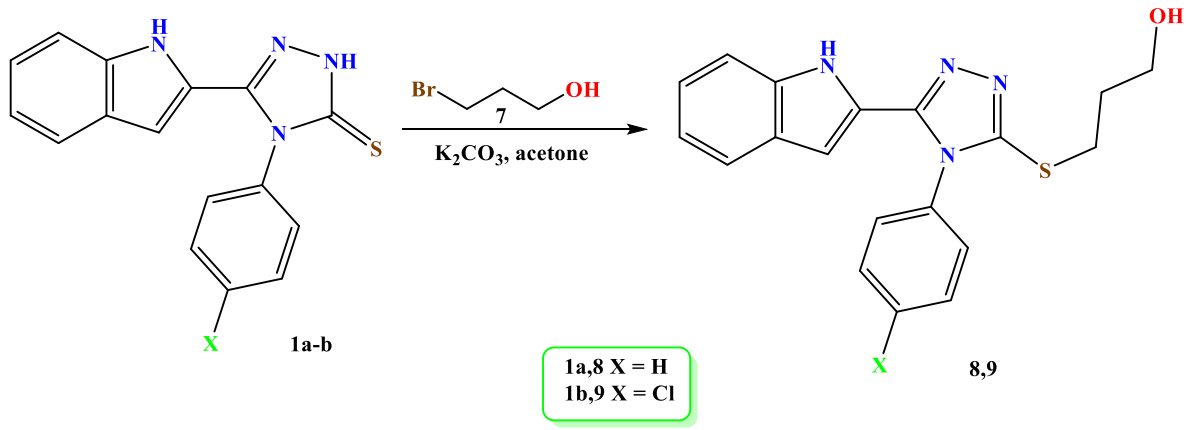

Scheme 2. Alkylation of **1a-b** with 3-bromopropanol.

3.2. Crystal Structure Description

Galactosyslation using a protected (acetylated) galctosyl subunit successfully afforded a good quality crystal suitable for X-ray single structure analysis. The structure of **5** was further confirmed using X-ray diffraction of a single crystal. The structure of the asymmetric unit is shown in Figure 1. As seen in this figure, there is one molecule of **5** as an asymmetric formula while four molecules are present in the unit cell. It crystallized in the orthorhombic crystal system and $P2_12_12_1$ space group. The unit cell parameters were a = 13.8302(6) Å, b = 13.8302(6) Å, and c = and 32.4134(19) Å (Table 1). The unit cell volume was 3087.1(3) Å^3, and the crystal density was 1.340 Mg/m^3. A summary of bond distances and angles is depicted in Table 2 and Table S1 (Supplementary Data). The phenyl and indole moieties were found to be twisted from the triazole ring mean plane by 66.24° and 18.86°, respectively. For the structurally related compound deposited as CCDC number 826844, the corresponding twist angles were 83.67° and 2.17°, respectively. In addition, the indole moiety was found rotated about 180° compared to that found in compound **5**, which could be attributed to the presence of a strong H-bonding interaction between the indole N-H and crystal water in the previously published structure.

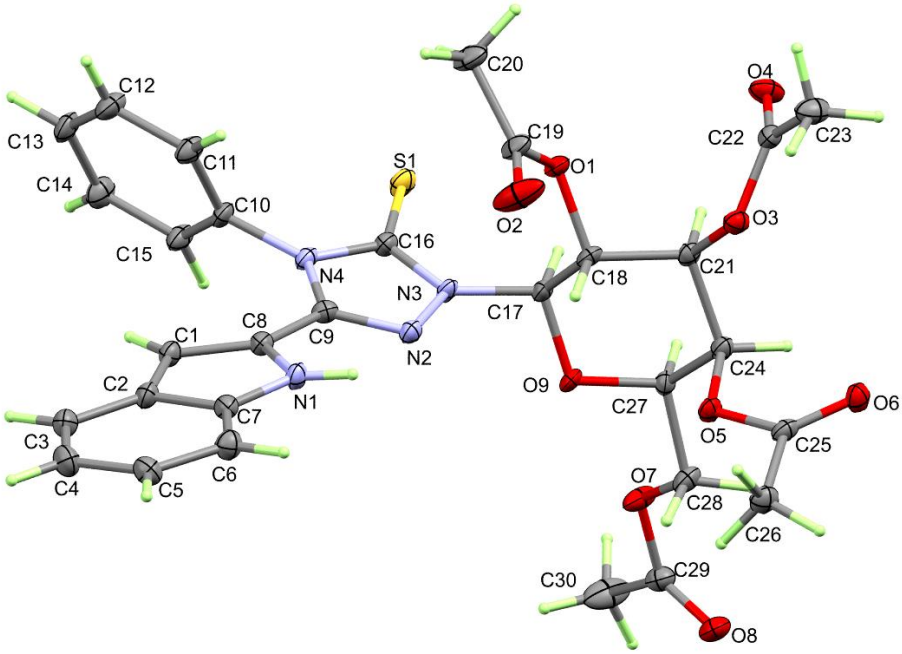

Figure 1. X-ray structure of **5**.

Table 2. Bond lengths (Å) for **5** and **9** [a].

Bond	Length/Å	Bond	Length/Å
5		**9**	
S(1)-C(16)	1.654(5)	Cl(1)–C(13)	1.741(3)
O(1)-C(19)	1.357(6)	N(15)–C(1)	1.371(3)
O(1)-C(18)	1.442(6)	N(15)–C(8)	1.382(3)
N(1)-C(7)	1.380(7)	N(16)–C(16)	1.370(3)
N(1)-C(8)	1.385(7)	N(16)–C(9)	1.377(3)
O(2)-C(19)	1.188(7)	N(16)–C(10)	1.444(3)
N(2)-C(9)	1.311(7)	N(17)–C(16)	1.315(3)
N(2)-N(3)	1.393(6)	N(17)–N(18)	1.399(3)
O(3)-C(22)	1.367(7)	N(18)–C(9)	1.311(3)
O(3)-C(21)	1.429(6)	C(16)–S(1)	1.732(3)

[a] List of bond angles are given in Table S1 (Supplementary Data).

The molecular units of **5** were connected by the O . . . H, N . . . H, and S . . . H interactions shown in Figure 2A. Details of these non-covalent forces are depicted in Table 3. The shortest O...H interaction was C(27)-H(27)...O(2) where the H-acceptor and donor(D)–acceptor(A) distances were 2.21 and 3.177(7) Å, respectively, while the donor–hydrogen–acceptor angle was 163.4°. In addition, the molecules' packing was controlled by C(23)-H(23B)...S(1) and C(30)-H(30C)...N(2) interactions where the D–A distances were 3.821(6) and 3.531(8) Å, respectively. The packing scheme of the molecular units is shown in Figure 2B.

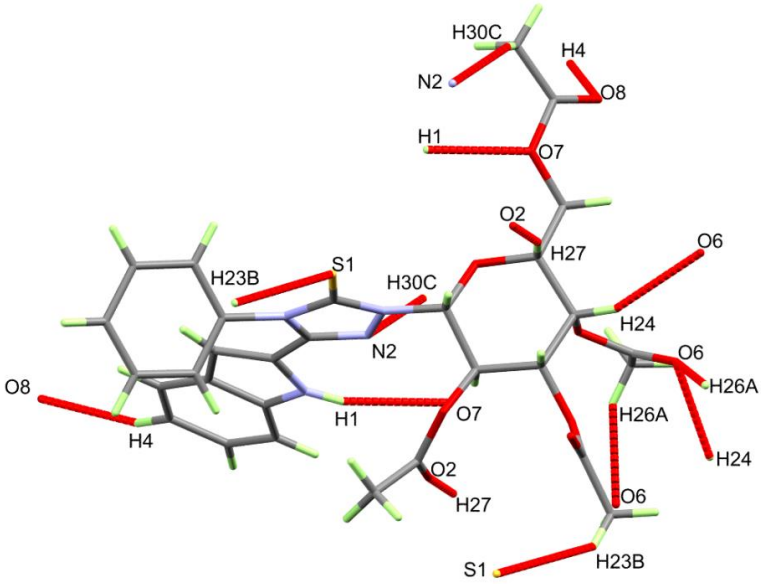

(**A**)

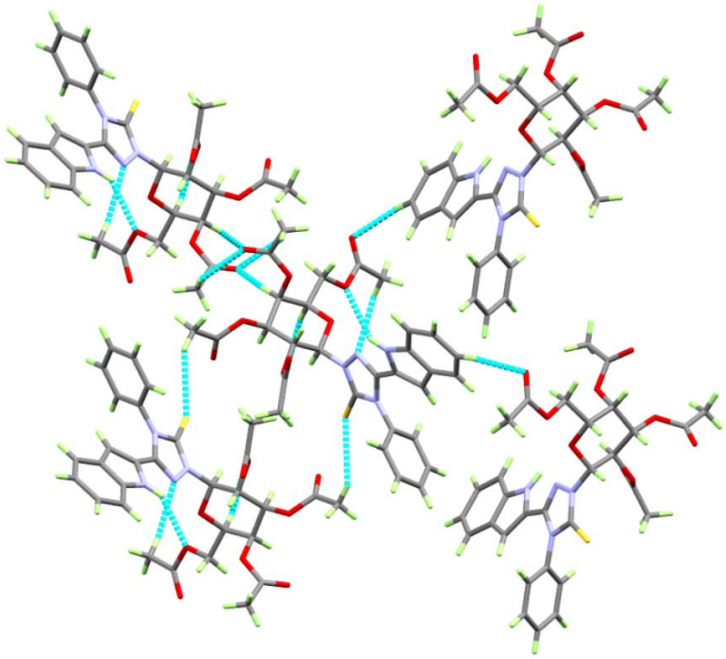

(**B**)

Figure 2. The N . . . H/S . . . H/O . . . H contacts (**A**) and molecular packing scheme (**B**) for **5**.

Table 3. Hydrogen bonds for **5** [Å and °].

D-H...A	d(D-H)	d(H...A)	d(D...A)	<(DHA)	Symm. Code
N(1)-H(1)...O(7)	0.85(6)	2.48(6)	3.238(6)	149(5)	x − 1, y, z
C(23)-H(23B)...S(1)	0.98	2.98	3.821(6)	144.8	x − 1/2, −y + 1/2, −z + 1
C(24)-H(24)...O(6)	1.00	2.47	3.416(6)	157.1	x + 1/2, −y + 3/2, −z + 1
C(26)-H(26A)...O(6)	0.98	2.56	3.290(7)	131	x − 1/2, −y + 3/2, −z + 1
C(27)-H(27)...O(2)	1.00	2.21	3.177(7)	163.4	x + 1, y, z
C(30)-H(30C)...N(2)	0.98	2.61	3.531(8)	156.2	x + 1, y, z

The X-ray structure of **9** is shown in Figure 3 while the detailed crystal data are given in Table 1. This compound crystallized in the less symmetric triclinic crystal system and *p-1* space group with unit cell parameters of a = 11.0384(5) Å, b = 13.6634(8) Å, c = 14.0630(6) Å, α = 74.579(4)°, β = 74.477(4), and γ = 72.100(5)°. There were two molecules as an asymmetric unit, and z = 4. The crystal density was 1.381 Mg/m^3, and the unit cell volume was 1905.31(18) Å^3. In this case, the twist angles between the triazole moiety and the phenyl or indole moieties were 73.15° and 20.70°, respectively. The respective values for the molecular unit with letter **B** in atom numbering were 77.29° and 13.96°, respectively. The most important bond distances and angles are depicted in Table 2 and Table S1 (Supplementary Data). For the structurally related compound reported by Dalimba et al. (CCDC No.: 913951), the corresponding twist angles are 73.38° and 81.53°, respectively [30].

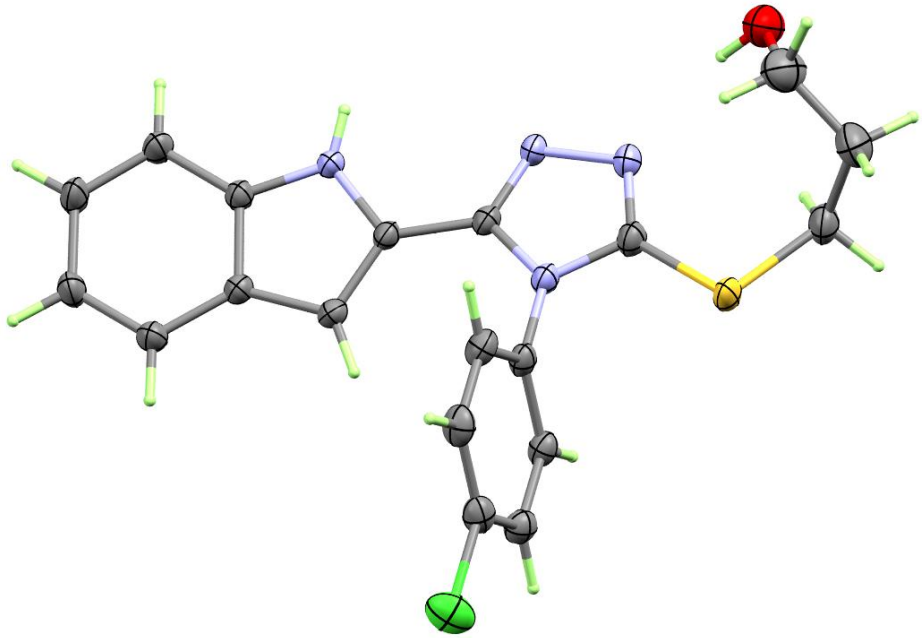

Figure 3. Structure with atom numbering for one of the two molecular units in the asymmetric formula of **9** drawn using 30% probability level for thermal ellipsoids.

3.3. Hirshfeld Surface Analysis

In the light of the importance of non-covalent interactions on crystal stability, the different contacts among molecular units were analyzed using Hirshfeld calculations. With the aid of Hirshfeld analysis, one can determine all possible non-covalent interactions and their percentages. The results presented in Figure 4 indicate that the H . . . H, O . . . H, C . . . H, and S . . . H intermolecular interactions were the most dominant. Their percentages were calculated to be 46.8%, 25.6%, 14.0%, and 6.3%, respectively.

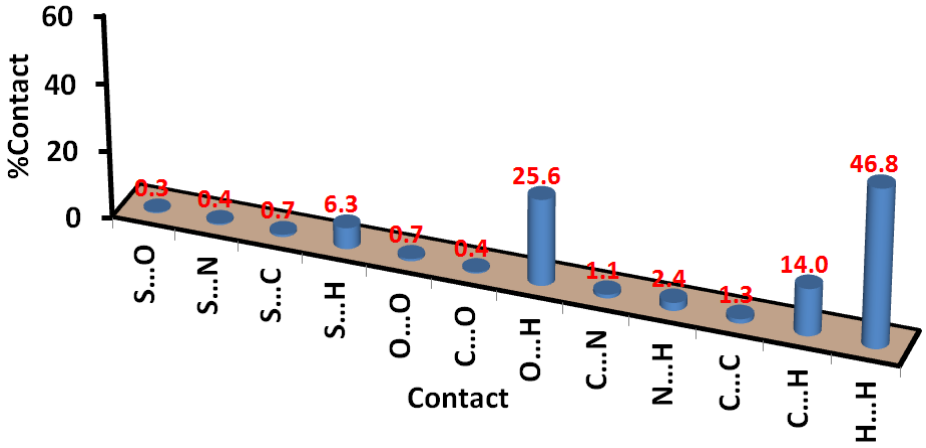

Figure 4. Intermolecular contacts and their percentages in **5**.

Hirshfeld surfaces such as d_{norm}, shape index, and curvedness maps are presented in Figure 5. In the d_{norm} map, there were many red spots indicating the presence of intermolecular contacts shorter than the vdWs radii sum of the interacting atoms. These red spots were found corresponding to the O . . . H, N . . . H, C . . . H, and S . . . H contacts, which are designated by letters A to D, respectively. Their percentages are depicted in Figure 4. Among these interactions, the O . . . H interactions were the most dominant. A summary of all short non-covalent interactions detected in the crystal structure of this compound with the aid of Hirshfeld analysis is listed in Table 4.

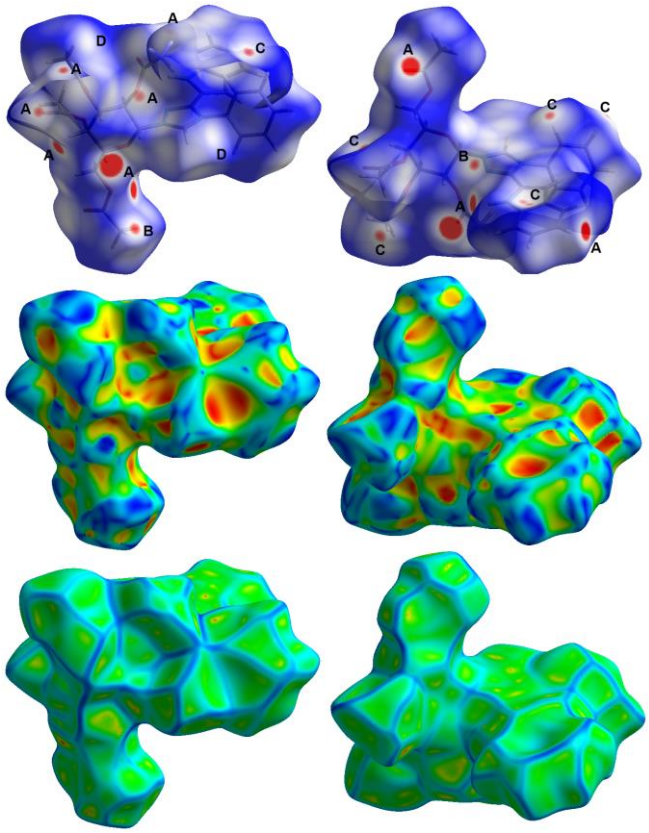

Figure 5. Hirshfeld surfaces of **5** showing the most important interactions (A) O . . . H, (B) N . . . H, (C) C . . . H, and (D) S . . . H.

Table 4. Short contacts and the corresponding interaction distances.

Contact	Distance	Contact	Distance
H1 . . . O7	2.607	H14 . . . C7	2.784
H6 . . . O7	2.348	H14 . . . C6	2.737
H24 . . . O6	2.396	H14 . . . C5	2.733
H26A . . . O6	2.497	H15 . . . C3	2.685
H26C . . . O8	2.606	H24 . . . C25	2.767
H27 . . . O2	2.126	H23A . . . C25	2.666
H30C . . . N2	2.518	H23A . . . C26	2.771
H11 . . . S1	3.025	H24 . . . C25	2.767

Careful inspection of the shape index and curvedness maps leaves no doubt about the absence of π–π stacking interactions. This observation agreed very well with the small contributions of the C . . . C (1.3%) and C . . . N (1.1%) interactions. Other interesting illustrations, which offer not only the weight of each contact in the crystal structure but also shed light on the strength of each contact, are the fingerprint plots shown in Figure 6. The area of the fingerprint gives the percentages of all contacts detected in the crystal structure. Hence, decomposition of the fingerprint gives the percentage of each contact in the crystal structure (Figure 4). In addition, the sharp spikes in the fingerprint plot indicate interactions with short distances and hence are important in molecular packing. This feature is clearly evident in the decomposed fingerprint plots of the H . . . S, H . . . O, H . . . C, and H . . . N interactions.

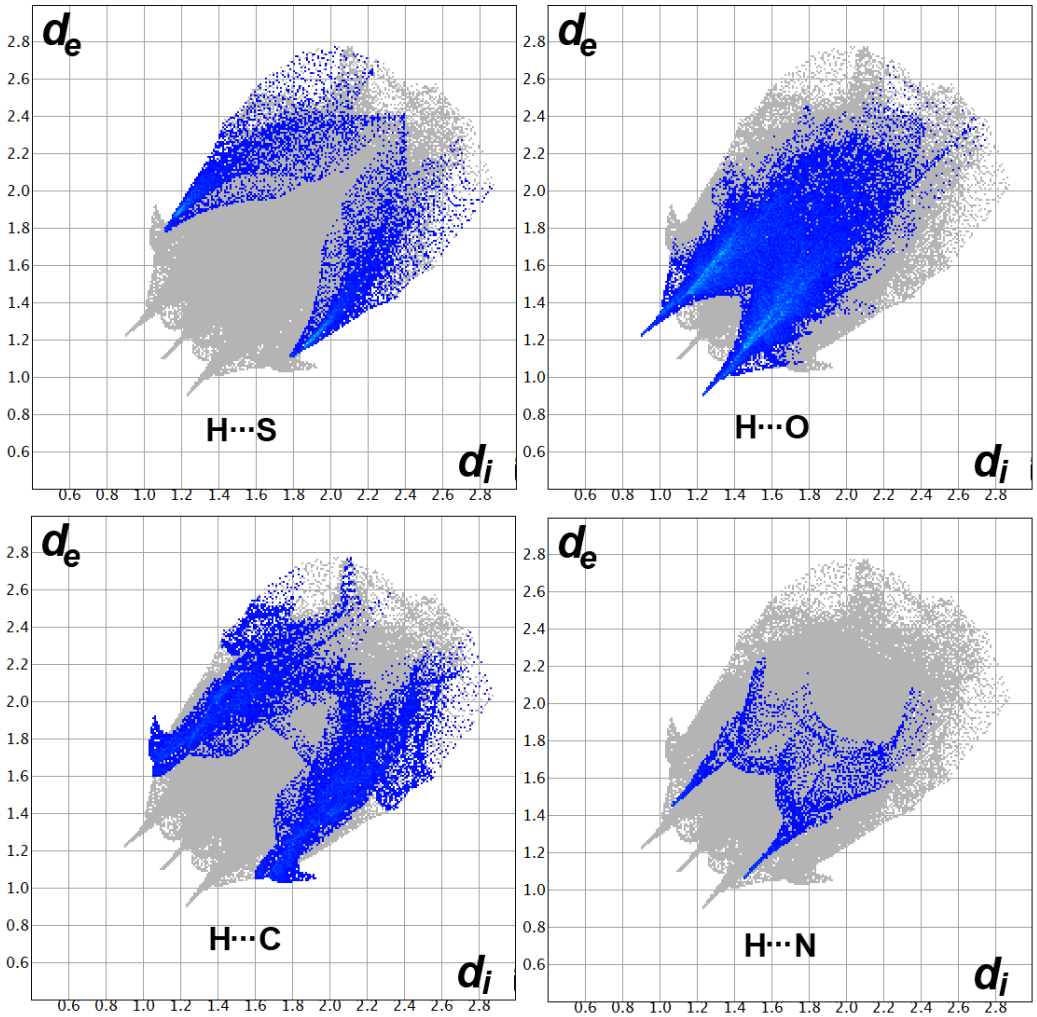

Figure 6. Decomposed fingerprint plots for the short contacts in **5**.

4. Conclusions

Base-dependent stereoselective β-galactosylation of 4-aryl-5-indolyl-1,2,4-triazole-3-thiones **1a** and **1b** were performed in the presence of $NaHCO_3$ to produce the *S*-galactosides **3,4** whereas the use of K_2CO_3 afforded a mixture of *S*- and *N*-galactosides **3-6**. Thermal migration of the galactosyl moiety from sulfur to nitrogen was successful using fusion, which was used to improve the yields of the *N*-galactosides. In addition, alkylation of **1a** and **1b** with 3-bromopropan-1-ol **7** in K_2CO_3 afforded the *S*-alkylated products **8** and **9**, respectively. NMR and single crystal analysis were used for structure determinations; two single crystals from compounds **5** and **9** were obtained, and their structural analyses were presented. The X-ray structure of **5** was used for analysis of molecular packing with the aid of Hirshfeld calculations. The supramolecular structure of **5** was found to depend on short O . . . H, N . . . H, C . . . H, and S . . . H contacts. Among these interactions, the O...H (25.6%) contacts were the most dominant while the N . . . H (2.4%), C . . . H (14.0), and S . . . H (6.3%) contributed less to molecular packing.

Supplementary Materials: The following supporting information can be downloaded at: https://www.mdpi.com/article/10.3390/cryst13050797/s1, Figures S1–S12: NMR spectrum; Table S1: Bond angles (°) for compounds **5** and **9**.

Author Contributions: Conceptualization, A.T.A.B., A.A. and A.B.; methodology, A.T.A.B. and A.A.; software, M.H., A.B., S.M.S. and M.S.A.; validation, A.T.A.B., A.A., A.B., S.M.S. and M.H.; formal analysis, A.A.; investigation, A.T.A.B., A.A., A.B., S.M.S. and M.H.; resources, A.T.A.B. and A.B.; data curation, M.H. and S.M.S.; writing—original draft preparation, S.M.S., A.T.A.B. and A.A.; writing—review and editing, A.T.A.B., A.A., A.B., S.M.S., M.S.A. and M.H.; visualization, A.A. and A.B.; supervision, A.T.A.B. and M.S.A.; funding acquisition, M.S.A. All authors have read and agreed to the published version of the manuscript.

Funding: Princess Nourah bint Abdulrahman University Researchers Supporting Project number (PNURSP2023R86), Princess Nourah bint Abdulrahman University, Riyadh, Saudi Arabia.

Data Availability Statement: Not applicable.

Acknowledgments: Princess Nourah bint Abdulrahman University Researchers Supporting Project number (PNURSP2023R86), Princess Nourah bint Abdulrahman University, Riyadh, Saudi Arabia.

Conflicts of Interest: The authors declare no conflict of interest.

References

1. Hayes, M.R.; Pietruszka, J. Synthesis of Glycosides by Glycosynthases. *Molecules* **2020**, *22*, 1434. [CrossRef] [PubMed]
2. Inman, M.; Moody, C.J. Indole synthesis-something old, something new. *Chem. Sci.* **2013**, *4*, 29–41. [CrossRef]
3. Berger, M.; Gray, J.A.; Roth, B.L. The expanded biology of serotonin. *Annu. Rev. Med.* **2009**, *60*, 355–366. [CrossRef] [PubMed]
4. Sharma, V.; Kumar, P.; Pathaka, D. Biological importance of the indole nucleus in recent years: A comprehensive review. *J. Heterocycl. Chem.* **2010**, *47*, 491–502. [CrossRef]
5. Zhang, M.Z.; Chen, Q.; Yang, G.F. A review on recent developments of indole-containing antiviral agents. *Eur. J. Med. Chem.* **2015**, *89*, 421–441. [CrossRef]
6. Frost, J.M.; Dart, M.J.; Tietje, K.R.; Garrison, T.R.; Grayson, G.K.; Daza, A.V.; El-Kouhen, O.F.; Yao, B.B.; Hsieh, G.C.; Pai, M.; et al. Indol-3-ylcycloalkyl ketones: Effects of N1 substituted indole side chain variations on CB2 cannabinoid receptor activity. *J. Med. Chem.* **2010**, *53*, 295–315. [CrossRef]
7. Rathod, A.S.; Godipurge, S.S.; Biradar, J.S. Microwave Assisted, Solvent-Free, "Green" Synthesis of Novel Indole Analogs as Potent Antitubercular and Antimicrobial Agents and Their Molecular Docking Studies. *Russ. J. Gen. Chem.* **2018**, *88*, 1238–1246. [CrossRef]
8. Niemyjska, M.; MacIejewska, D.; Wolska, I.; Truszkowski, P. Synthesis, structural investigations, and anti-cancer activity of new methyl indole-3-carboxylate derivatives. *J. Mol. Struct.* **2012**, *1026*, 30–35. [CrossRef]
9. Aggarwal, R.; Sumran, G. An Insight on Medicinal Attributes of 1,2,4-Triazoles. *Eur. J. Med. Chem.* **2020**, *205*, 112652. [CrossRef]
10. Kaur, R.; Ranjan Dwivedi, A.; Kumar, B.; Kumar, V. Recent Developments on 1,2,4-Triazole Nucleus in Anticancer Compounds: A Review. Anti-Cancer Agents. *Med. Chem.* **2016**, *16*, 465–489.
11. Wen, X.; Zhou, Y.; Zeng, J.; Liu, X. Recent Development of 1,2,4-Triazole-Containing Compounds as Anticancer Agents. *Curr. Top. Med. Chem.* **2020**, *20*, 1441–1460. [CrossRef] [PubMed]
12. Shaker, R.M. The Chemistry of Mercapto- and Thione-Substituted 1,2,4-Triazoles and Their Utility in Heterocyclic Synthesis. *Arkivoc* **2006**, *9*, 59–112. [CrossRef]

13. Slivka, M.V.; Korol, N.I.; Fizer, M.M. Fused Bicyclic 1,2,4-triazoles with One Extra Sulfur Atom: Synthesis, Properties, and Biological Activity. *J. Heterocycl. Chem.* **2020**, *57*, 3236–3254. [CrossRef]
14. Küçükgüzel, Ş.G.; Çıkla-Süzgün, P. Recent Advances Bioactive 1,2,4-Triazole-3-Thiones. *Eur. J. Med. Chem.* **2015**, *97*, 830–870. [CrossRef]
15. Patel, K.R.; Brahmbhatt, J.G.; Pandya, P.A.; Daraji, D.G.; Patel, H.D.; Rawal, R.M.; Baran, S.K. Design, Synthesis and Biological Evaluation of Novel 5-(4-Chlorophenyl)-4-Phenyl-4H-1,2,4-Triazole-3-Thiols as an Anticancer Agent. *J. Mol. Struct.* **2021**, *1231*, 130000. [CrossRef]
16. Su, L.; Feng, Y.; Wei, K.; Xu, X.; Liu, R.; Chen, G. Carbohydrate-Based Macromolecular Biomaterials. *Chem. Rev.* **2021**, *121*, 10950–11029. [CrossRef]
17. Borai, A.T.A.; Gomaa, M.S.; El Ashry, E.S.H.; Duerkop, A. Design, Synthesis, X-ray Crystal Structure and Regioselectivity Determination of Dihydro-Indolyl-1,2,4-triazole-3-thione and its 3-Benzylsulfanyl Analogues as Potent Anticancer Agents. *Eur. J. Med. Chem.* **2017**, *125*, 360–371. [CrossRef]
18. Boraei, A.T.A.; Singh, P.K.; Sechi, M.; Satta, S. Discovery of novel functionalized 1,2,4-triazoles as PARP-1 inhibitors in breast cancer: Design, synthesis and antitumor activity evaluation. *Eur. J. Med. Chem.* **2019**, *182*, 111621. [CrossRef]
19. Nafie, M.S.; Boraei, A.T.A. Exploration of novel VEGFR2 tyrosine kinase inhibitors via design and synthesis of new alkylated indolyl-triazole Schiff bases for targeting breast cancer. *Bioorg. Chem.* **2022**, *122*, 105708. [CrossRef]
20. Youssef, M.F.; Nafie, M.S.; Salama, E.E.; Boraei, A.T.A.; Gad, E.M. Synthesis of New Bioactive Indolyl-1,2,4-Triazole Hybrids as Dual Inhibitors for EGFR/PARP-1 Targeting Breast and Liver Cancer Cells. *ACS Omega* **2022**, *7*, 45665–45677. [CrossRef]
21. Al-Hussain, S.A.; Farghaly, T.A.; Zaki, M.E.A.; Abdulwahab, H.G.; Al-Qurashi, N.T.; Muhammad, Z.A. Discovery of novel indolyl-1,2,4-triazole hybrids as potent vascular endothelial growth factor receptor-2 (VEGFR-2) inhibitors with potential anti-renal cancer activity. *Bioorg. Chem.* **2020**, *105*, 104330. [CrossRef] [PubMed]
22. Maftei, C.V.; Fodor, E.; Jones, P.G.; Daniliuc, C.G.; Franz, M.H.; Kelter, G.; Fiebig, H.; Tamm, M.; Neda, I. Novel 1,2,4-oxadiazoles and trifluoromethylpyridines related to natural products: Synthesis, structural analysis and investigation of their antitumor activity. *Tetrahedron* **2016**, *72*, 1185–1199. [CrossRef]
23. Neda, I.; Sakhaii, P.; Waßmann, A.; Niemeyer, U.; Günther, E.; Engel, J. A practical synthesis of benzyl α- and allyl β-D-glucopyranosides regioselectively substituted with $(CH_2)_3OH$ groups: Stereocontrolled β-galactosidation by cation π-interaction. *Synthesis* **1999**, *9*, 1625–1632. [CrossRef]
24. Rikagu Oxford Diffraction. *CrysAlisPro*; Rikagu Oxford Diffraction Inc.: Yarnton, UK, 2022.
25. Sheldrick, G.M. SHELXT-Integrated space-group and crystal-structure determination. *Acta Cryst.* **2015**, *A71*, 3–8. [CrossRef]
26. Sheldrick, G.M. Crystal Structure Refinement with SHELXL. *Acta Cryst.* **2015**, *C71*, 3–8.
27. Hübschle, C.B.; Sheldrick, G.M.; Dittrich, B. *ShelXle*: A Qt graphical user interface for *SHELXL*. *J. Appl. Crystallogr.* **2011**, *44*, 1281–1284. [CrossRef]
28. Dolomanov, O.V.; Bourhis, L.J.; Gildea, R.J.; Howard, J.A.K.; Puschmann, H.J. OLEX2: A complete structure solution, refinement and analysis program. *Appl. Cryst.* **2009**, *42*, 339–341. [CrossRef]
29. Turner, M.J.; McKinnon, J.J.; Wolff, S.K.; Grimwood, D.J.; Spackman, P.R.; Jayatilaka, D.; Spackman, M.A. Crystal Explorer17 (2017) University of Western Australia. Available online: https://crystalexplorer.net/ (accessed on 30 July 2020).
30. Panathur, N.; Dalimba, U.; Koushik, P.V.; Alvala, M.; Yogeeswari, P.; Sriram, D.; Kumar, V. Identification and characterization of novel indole based small molecules as anticancer agents through SIRT1 inhibition. *Eur. J. Med. Chem.* **2013**, *69*, 125–138. [CrossRef]